Journal of Power Sources 199 (2012) 46–52

Contents lists available at SciVerse ScienceDirect

Journal of Power Sources

journal homepage: www.elsevier.com/locate/jpowsour

Rotating disk electrode measurements of activity and stability of monolayer Pt on tungsten carbide disks for oxygen reduction reaction

Irene J. Hsu[a], Yannick C. Kimmel[a], Yu Dai[b], Shengli Chen[b], Jingguang G. Chen[a,*]

[a] Department of Chemical Engineering, University of Delaware, Newark, DE 19716, United States
[b] Hubei Key Laboratory of Electrochemical Power Sources, Department of Chemistry, Wuhan University, Wuhan 430072, China

ARTICLE INFO

Article history:
Received 10 August 2011
Received in revised form 7 October 2011
Accepted 9 October 2011
Available online 14 October 2011

Keywords:
Platinum
Tungsten carbide
Oxygen reduction reaction
Tungsten oxidation
Rotating disk electrode measurements

ABSTRACT

In the current study, rotating disk electrode measurements were performed to gain insight into the oxygen reduction reaction (ORR) performance of Pt supported on single-phase tungsten monocarbide (WC) substrates. Using well-defined WC disks with precise Pt depositions, the interaction between Pt and WC can be studied during the ORR without any additional complexities, such as support effects and uncertainties regarding the direct contact of Pt with WC. Furthermore, XPS is used to determine the surface concentration and oxidation state of WC and Pt before and after ORR measurements, showing how the catalyst is affected during the ORR. The monolayer Pt on WC system shows smaller than expected activities compared to bulk Pt. The cause for the depressed activity is attributed to the formation of tungsten oxides under excess oxygen and high oxidizing potentials during the ORR. The presence of tungsten oxides are confirmed by XPS, and its effect on the stability of the monolayer Pt and WC system is further demonstrated with voltammetric results. These results clarify some unresolved issues with the current literature regarding the synergistic effect between Pt and WC in the ORR.

1. Introduction

The mass commercialization of low-temperature proton exchange membrane (PEM) fuel cells is impeded partially by its high cost, some of which is due to the expense of the precious metal catalyst. Platinum (Pt) catalysts are commonly used to aid reactions taking place in both the anode and the cathode of the hydrogen PEM fuel cell. In order to make fuel cells more economically viable, the amount of Pt used in these reactions must be significantly reduced. In particular, the oxygen reduction reaction (ORR), which takes place in the cathode, is a reaction with sluggish kinetics. Even with the aid of Pt catalysts, the ORR kinetics are fairly slow, which results in large overpotential losses and prevents the maximum overall fuel cell efficiency from being achieved. Therefore, significant research efforts have been devoted to finding new catalysts that can improve the ORR performance while reducing Pt loadings.

Using density functional theory (DFT) calculations to determine the atomic oxygen binding energy (O_{BE}), Norskov et al. have established that the value of O_{BE} is a useful descriptor to predict the ORR activity of a catalyst [1]. While Pt is confirmed to be the highest performing monometallic catalyst for this reaction [1], other catalytic systems have been discovered using this method. For example, Adzic and co-workers have reported that monolayer Pt systems show promise in making highly active catalysts for ORR while reducing the Pt loading considerably [2–4]. While success has been shown in reducing Pt, the substrates in these studies are also precious metals. There are cost advantages to the observed higher activities, but it would be even more beneficial to support monolayer Pt on substrates that are less costly and more abundant. Transition metal carbides, and in particular tungsten monocarbide (WC), have received some attention as possible support materials as well as replacements for precious metals for electrochemical catalytic applications. WC is three orders of magnitude less costly than Pt and other precious metals [5] and has been shown to be stable under a fairly wide potential range under acidic conditions [6]. Furthermore, monolayer Pt on WC (ML Pt/WC) has been shown to be promising in replacing bulk Pt catalysts for the hydrogen evolution reaction (HER) [5] and methanol oxidation reaction [7–9]. DFT calculations have previously shown that the O_{BE} for WC(0 0 0 1) is almost twice as strong as that for Pt(1 1 1), predicting that WC should not be a good ORR catalyst [10]. However, when one monolayer of Pt is added onto the WC(0 0 0 1) surface, the resulting O_{BE} is nearly equivalent to that of Pt(1 1 1) [10]. Therefore, ML Pt/WC is predicted to be a good ORR catalyst with activity that is similar to bulk Pt. A similar trend was observed for HER – while the

* Corresponding author. Tel.: +1 302 831 0642; fax: +1 302 831 2085.
E-mail address: jgchen@udel.edu (J.G. Chen).

0378-7753/$ – see front matter © 2011 Elsevier B.V. All rights reserved.
doi:10.1016/j.jpowsour.2011.10.024

hydrogen binding energy on the WC(0 0 0 1) surface was very strong, the addition of a Pt monolayer reduced the binding energy to levels very similar to that of Pt(1 1 1) [5]. Electrochemical measurements then confirmed the DFT predictions of similar HER activity between ML Pt/WC and bulk Pt [5], thereby demonstrating the usefulness of this catalyst design methodology as well as the potential of the ML Pt/WC catalyst to replace bulk Pt.

Previous work in the literature has also identified the Pt–WC system as a promising ORR catalyst. They have shown that the ORR activity is enhanced when Pt particles are combined with WC and W_2C powders supported on high surface area carbon [11–22]. In addition, Pt stability on WC has been shown to be greater than on carbon. The reason for the increased stability has been attributed to a stronger interaction between Pt and WC over that between Pt and carbon, making WC a promising support material over carbon [23,24].

However, these studies use powder systems that are supported on high surface area carbon, making it difficult to discern whether Pt atoms reside directly on top of the WC particles or the carbon substrate. To tie together the DFT findings and the promising results seen in the literature, studies on well-characterized ML Pt/WC thin films are necessary to ensure direct interaction between Pt atoms and the WC substrate. Additionally, the Pt loadings used in the literature are generally quite high (>20 wt.%), and the question of whether the amount of Pt can be reduced to monolayer amounts, as predicted by DFT calculations, remains. In the current work we aim to test the possibility of using monolayer Pt on WC as an ORR catalyst by undertaking rotating disk electrode (RDE) studies using WC films prepared on a W disk. The use of the well-defined surfaces of WC, ML Pt/WC, and bulk Pt disks allows comparisons on the basis of geometric surface area. Results from the current study can provide useful insight into the ORR activity and stability of Pt/WC without additional complexities such as particle size, the presence of a carbon support, or excess impurities.

2. Experimental methods

A 5 mm diameter RDE tungsten disk (Pine) and a tungsten foil were converted to WC by annealing in a quartz tube furnace at 1000 °C under a hydrogen and methane environment, as described previously [6]. A Pt monolayer was then thermally evaporated onto the WC disk under ultrahigh vacuum (UHV) conditions using a Pt wire wrapped around a resistively heated tungsten filament. XPS (PHI-5600 system with an Al Kα X-ray source and hemispherical detector) was used to confirm the presence one monolayer of Pt on the WC substrate based on overlayer calculations [5]. An RDE Pt disk (5 mm, Pine) was used as received. Prior to electrochemical testing, the disks were cleaned by polishing with 0.05 μm alumina and sonicating for about 1 h. Surface W-oxides were removed prior to electrochemical testing by briefly submerging the WC disk samples in 0.3 M NaOH.

The ORR activity measurements were performed in a three-electrode cell using an interchangeable RDE system (Pine Instruments) and a Princeton Applied Research potentiostat/galvanostat model VersaSTAT 4 at room temperature. A Pt wire was used as the counter electrode and a saturated calomel electrode (SCE) was used as the reference, although all results are reported herein are with respect to the normal hydrogen electrode (NHE). Samples were first electrochemically conditioned in nitrogen-purged 0.5 M H_2SO_4 by cycling for about 30 min from 0 V to the onset of oxidation at 100 mV s^{-1} for the WC and Pt/WC disks and 0–1.4 V at 100 mV s^{-1} for the Pt disk. Following that, the electrolyte solution was purged with oxygen for 30 min, and 20 cycles were completed in the O_2-saturated solution at 100 mV s^{-1}. Linear scan voltammograms were then taken at a range of rotation speeds and a scan rate of 10 mV s^{-1}.

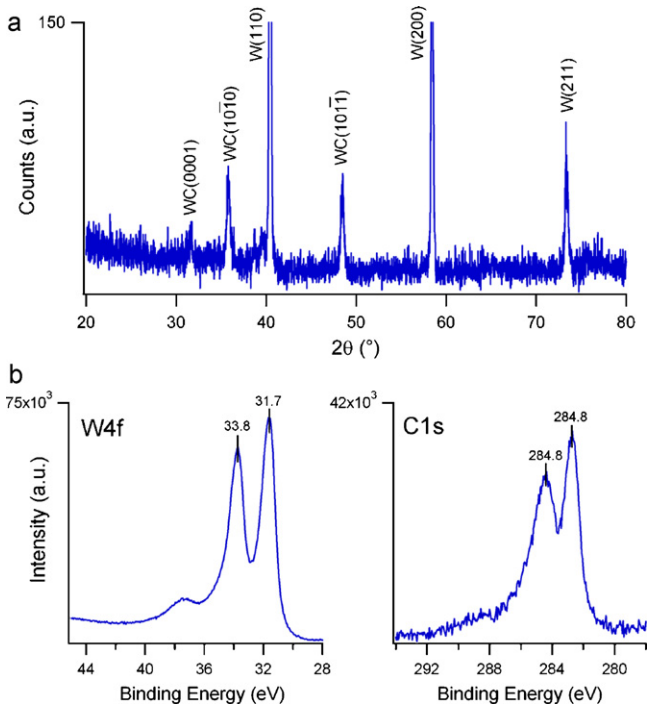

Fig. 1. (a) XRD pattern of the WC disk confirming single phase WC and (b) XPS scans showing W4f and C1s regions of the WC disk.

3. Results and discussion

3.1. Comparison of ORR activity of WC, Pt, and ML Pt/WC

Polycrystalline WC disks are used as model surfaces to determine the effects of the Pt monolayer without additional complexities seen in the literature thus far. Results using the ML Pt/WC disks can also be compared to the polycrystalline Pt disk as a reference. XRD confirms that the WC layer is single phase (Fig. 1a). The W substrate peaks dominate the XRD pattern because the WC layer makes up only the top ~100 nm of the disk surface based on glancing incidence XRD [5]. XPS scans showing the W4f and C1s regions (Fig. 1b) confirm that the surface is WC with minimal free carbon (peak at 284.8 eV). The W4f $_{7/2}$ peak at 31.7 eV, W4f $_{5/2}$ peak at 33.8 eV, and carbidic carbon peak at 282.8 eV are characteristic of a WC surface. The W:C atomic ratio determined from these XPS peaks is approximately 1.1, in agreement with previous findings [5].

Fig. 2 shows cyclic voltammograms (CV) for the ML Pt/WC and WC disks in (a) N_2-saturated 0.5 M H_2SO_4 and (b) O_2-saturated 0.5 M H_2SO_4. The CV curves were recorded using a scan rate of 100 mV s^{-1} and the 20th cycles are shown. To minimize irreversible WC oxidation, the upper potential limit for cycling is restricted to 0.8 V for WC and 0.9 V for ML Pt/WC. Some oxidation is observed in the ML Pt/WC sample as noted by the sharp rise in current after 0.8 V. The existence of Pt on the ML Pt/WC sample is confirmed with the features present in the hydrogen adsorption region at low potentials (0–0.4 V). Conversely, no such peaks are seen on the WC sample. The magnitudes of the currents in the double layer region for both disk samples are comparable, indicating that the electrode surfaces have similar roughness [25]. In Fig. 2b, the O_2 reduction peak is observed for ML Pt/WC at around 0.4 V. The equilibrium potential for the oxygen reduction reaction is 1.23 V vs. NHE, and bulk Pt has a peak potential at around 0.6 V under the same

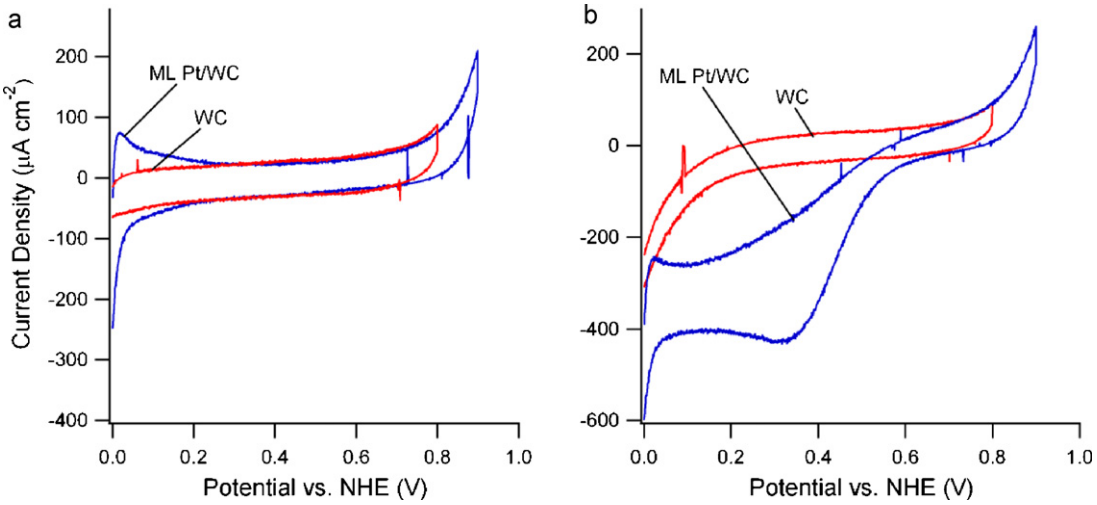

Fig. 2. Cyclic voltammograms of WC and ML Pt/WC in (a) N_2-saturated and (b) O_2-saturated 0.5 M H_2SO_4. Scan rate 100 mV s^{-1}, 20th cycle shown.

experimental conditions. In contrast, the WC disk does not exhibit any features associated with ORR.

Fig. 3 shows positive-going linear scan voltammograms (LSV) in an O_2-saturated 0.5 M H_2SO_4 electrolyte for WC, ML Pt/WC, and Pt disks using a rotation rate of 1600 rpm. The LSV for WC remains flat throughout the potential region between 0 and 0.8 V, indicating that WC shows no activity towards ORR, similar to what was observed in the CV in O_2-saturated environments. After 0.8 V, a sharp rise in current is observed due to the irreversible oxidation of the WC at the higher potential. The same curvature is also seen with ML Pt/WC, showing that there is also tungsten oxidization at the high potential. Some activity is observed with ML Pt/WC with an onset potential at around 0.5 V and a half-wave potential at ~0.3 V. This is almost 0.5 V more negative than that of bulk Pt, which shows the highest activity of the three disk samples.

The DFT calculations discussed earlier correctly predict the inactive nature of WC due to the high O_{BE} value. More interestingly, Fig. 3 shows that ML Pt/WC is considerably less active than Pt, which contradicts results from the same calculations of similar O_{BE} values on the two surfaces. However, DFT calculations use idealized single crystal surfaces to determine the O_{BE}. The ORR kinetics are very sensitive to the catalyst surface condition, and the oxidation

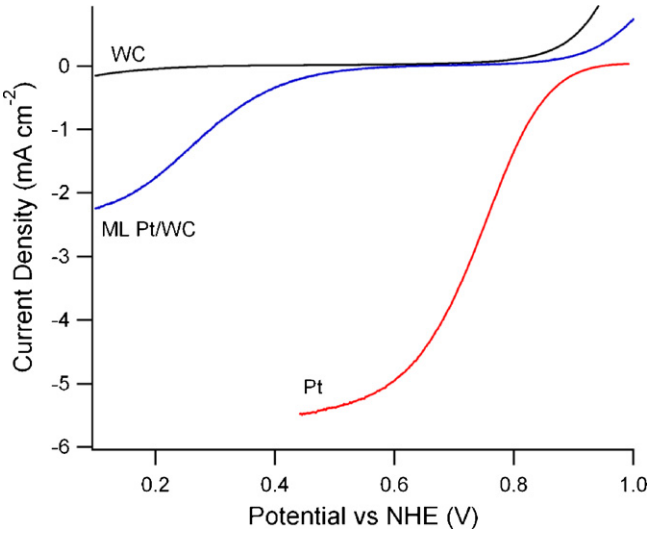

Fig. 3. O_2 reduction polarization curves for WC, ML Pt/WC, and bulk Pt in O_2-saturated 0.5 M H_2SO_4. Scan rate 10 mV s^{-1}; rotation speed 1600 rpm.

state of a surface is known to adversely affect the extent of activity. Furthermore, the WC surface can be oxidized in atmosphere [26] as well as at potentials higher than 0.8 V [6]. The irreversible electrochemical oxidation of WC is demonstrated in both Figs. 2 and 3. The fuel cell cathode operating potential range is between 0.6 and 1.1 V, and W-oxides are most likely to exist in this region [6].

XPS measurements before and after the ORR measurements confirm the formation of W-oxides during the reaction (Fig. 4a). Before ORR the W4f peaks can be attributed to WC, with the $4f_{7/2}$ at 31.8 eV, the $4f_{5/2}$ peak at 33.9 eV, and the $5p_{3/2}$ peak at 37 eV [27]. When W-oxidation occurs, oxidized W peaks appear at 35.9 eV and 38.0 eV. In this case, the oxide peaks are quite small and are visible after the spectral subtraction to reveal the difference between spectra before and after the ORR measurements, as demonstrated in Fig. 4a. The ratios of W-oxide to WC peaks were determined based on the normalized intensities of these peaks and are displayed in Table 1. The WC sample shows slightly more oxidation than ML Pt/WC, but still only about 36% of the WC is converted into the oxidized state during the ORR measurements. The Pt on the ML Pt/WC sample remains metallic, as indicated by the constant Pt4f peak positions in the spectra in Fig. 4b. The Pt4f peaks on the ML Pt/WC sample are slightly shifted from the bulk Pt peaks located at 71.2 and 74.5 eV. This shift has been observed previously for monolayer Pt [5]. The absence of oxidized Pt in ML Pt/WC indicates that the monolayer Pt does not seem to be more susceptible to oxidation than bulk Pt.

3.2. Comparison between ML Pt/WC and thick Pt/WC

To determine how larger Pt loadings on WC affect the ORR activity, a thicker Pt film was evaporated onto the WC disk. The thickness of the Pt film was estimated to be approximately 6 monolayers using XPS and overlayer calculations. The XPS survey scan in Fig. 5a compares the Pt4f and W4f peak for both the monolayer Pt and the thick Pt samples. When a thicker Pt film on the WC disk is used, the ORR polarization curve appears to be similar to that of the ML Pt/WC curve rather than bulk Pt.

Fig. 5b shows the ORR LSV curves for both ML Pt/WC and thick Pt/WC. The thick Pt/WC sample behaves more similarly to the ML Pt/WC sample rather than bulk Pt. The thick Pt/WC disk has the same limiting current as the ML Pt/WC disk, but the half-wave potential of ORR is about 0.1 V more positive than that for ML Pt/WC. The smaller overpotential is due to the increased Pt on the WC, but the half-wave potential for both the ML Pt/WC and the thick Pt/WC are considerably more negative than that for bulk Pt. It is likely that

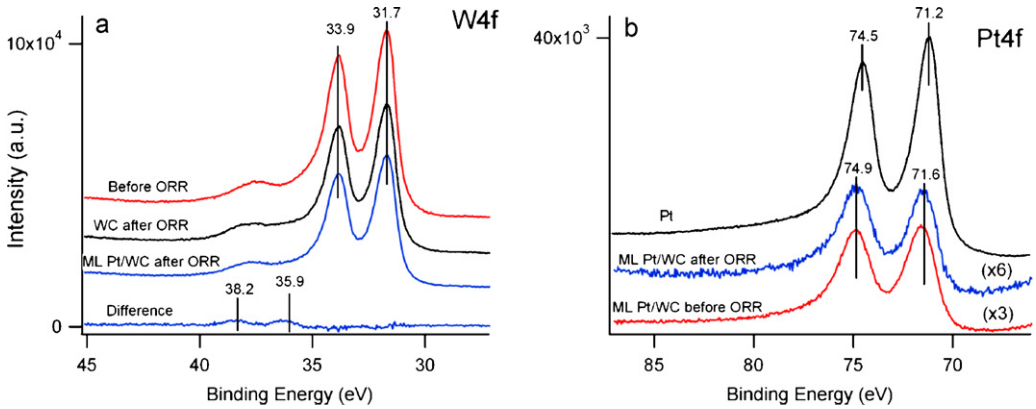

Fig. 4. XPS scans of the (a) W4f and (b) Pt4f regions for WC, ML Pt/WC, and Pt before and after O_2 reduction polarization measurements.

Table 1
XPS percentage changes after O_2 reduction LSV measurements.

% WO_x WC	% WO_x ML Pt/WC	% WO_x thick Pt/WC	% Change Pt:W ML Pt/WC	% Change Pt:W Thick Pt/WC
36	26	25	−63	−11

the thick Pt/WC sample behaves differently from bulk Pt because the oxidation of the WC substrate alters the Pt above it. Another explanation is that the growth of Pt does not follow the layer-by-layer mechanism, allowing exposed WC to oxidize easily. The XPS analysis in Table 1 shows that the WC substrate experiences the same extent of oxidation with the thick Pt overlayer as the ML Pt following the same O_2 reduction measurement sequence.

However, CV curves in O_2-saturated 0.5 M H_2SO_4 before and after the O_2 reduction polarization measurements show different trends for the ML Pt/WC and thick Pt/WC samples (Fig. 6). Before the measurements were taken, the general shapes of the CVs are similar for both samples (Fig. 6a). When CVs were taken after O_2 reduction LSVs, the peak current for the ML Pt/WC CV decreased and the peak potential shifted to more negative values, while the CV for thick Pt/WC remained relatively unchanged (Fig. 6b). The thick Pt/WC sample, therefore, shows greater stability than the ML Pt/WC sample, which declined in activity as the measurements continued. The more negative half-wave potential for the ML Pt/WC sample seen in Fig. 5b can be attributed to the instability of the Pt/WC surface during the measurement. The Pt:W XPS intensity ratios for both the ML Pt/WC and the thick Pt/WC samples were also determined before and after the ORR polarization measurements and are also displayed in Table 1. A change in Pt:W ratio is observed before and after the O_2 reduction polarization measurements for both samples, but there is a larger reduction in Pt observed with the ML Pt/WC sample compared to thick Pt/WC. Changes in the Pt:W ratio suggest that the structure of the Pt layer changes during the O_2 reduction reaction. Therefore, although the WC substrate oxidizes during the O_2 reduction for both ML Pt/WC and thick Pt/WC, the CV and XPS results show that the thick Pt/WC is able to maintain its initial overlayer structure better than the ML Pt/WC surface.

Because the thick Pt/WC was found to be more stable than the ML Pt/WC, multiple ORR polarization curves could be measured at varying rotation speeds (Fig. 7a). Koutecky–Levich plots for O_2 reduction were then generated for a range of potentials (Fig. 7b), showing curves that are linear and parallel over a wide potential range. These plots use the principle that the measured current is equivalent to the kinetic current and the limiting current (i_l), as described in Eq. (1).

$$\frac{1}{i} = \frac{1}{i_k} + \frac{1}{i_l} = \frac{1}{i_k} + \frac{1}{B\omega^{1/2}} \quad (1)$$

The intercept of the Koutecky–Levich plot is the inverse of the kinetic current ($1/i_k$), while the slope is $1/B$. The number of electrons transferred during reaction can then be calculated from B using Eq. (2) and the following constants: Faraday constant, $F = 96{,}489\ \mathrm{C\ mol^{-1}}$; geometric surface area $A = 0.196\ \mathrm{cm^2}$ for a 5 mm diameter disk electrode; diffusivity of oxygen in 0.5 M H_2SO_4,

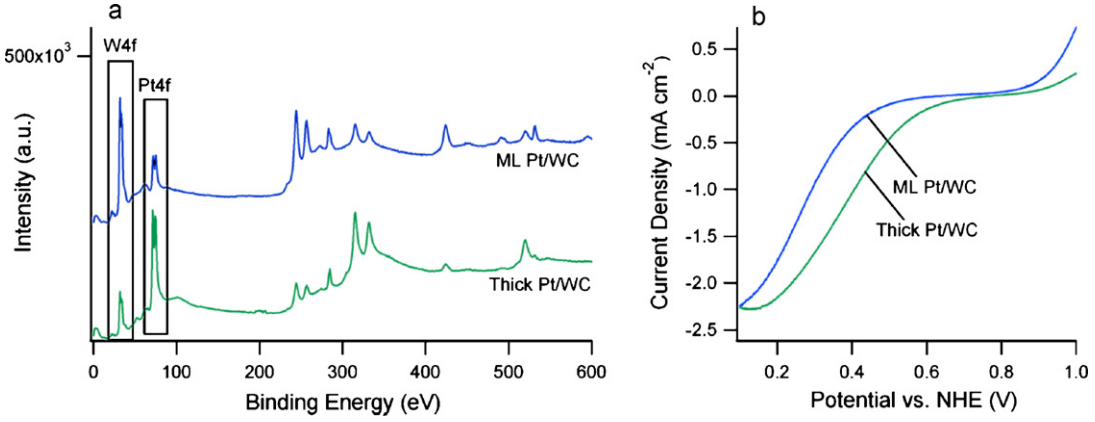

Fig. 5. (a) XPS survey scans for ML Pt/WC and Thick Pt/WC and (b) polarization curves for ML Pt/WC and Thick Pt/WC in O_2-saturated 0.5 M H_2SO_4.

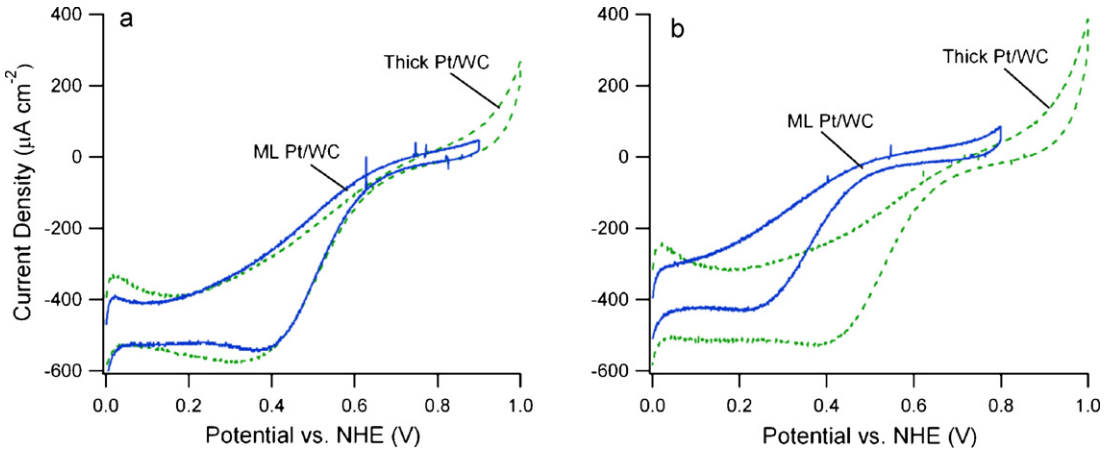

Fig. 6. CV in O_2-saturated 0.5 M H_2SO_4 (a) before and (b) after O_2 reduction polarization measurements for both ML Pt/WC and thick Pt/WC.

$D_{O_2} = 1.4 \times 10^{-5}$ cm^2 s^{-1} [19]; kinematic viscosity, $\nu = 0.010$ cm^2 s^{-1} [19]; saturated concentration of O_2 in 0.5 M H_2SO_4, $C_{O_2} = 1.1 \times 10^{-5}$ mol cm^{-3} [19].

$$B = 0.62nFAD_{O_2}^{2/3}\nu^{-1/6}C_{O_2} \quad (2)$$

Using this equation, the number of transferred electrons, n, was calculated to be 2.6 for all potentials featured in the Koutecky–Levich plots in Fig. 7b. This observation suggests that a 2-electron reduction process takes place for the Pt/WC surfaces, with oxygen reducing to H_2O_2 prior to reducing completely to H_2O. Because the limiting currents of ML Pt/WC and thick Pt/WC are similar, it can be implied that the 2-electron conversion to H_2O_2 also takes place on ML Pt/WC. Using the same analysis for the bulk Pt disk, the number of electrons transferred was calculated to be approximately 4, which is in agreement with the literature [25].

3.3. *Effect of WC oxidation on Pt monolayer stability and O_2 reduction activity*

In the calculation of the O_{BE} by DFT, a clean WC(0 0 0 1) surface is used, but the results of this study indicate that the WC surface becomes oxidized under ORR conditions. It seems that the unexpectedly low O_2 reduction activity seen with ML Pt/WC stems from changes taking place on the WC surface. Further evidence of this is observed when a ML Pt/WC foil is cycled between 0.0 and 1.0 V in O_2-saturated 0.5 M H_2SO_4 (Fig. 8a). The upper potential reaches oxidizing potentials, leading to WC oxidation after each CV cycle. With increasing number of cycles, the oxidation peak at potentials greater than 0.8 V shifts upwards while the O_2 reduction peak shifts to lower potentials, as indicated by the arrows. Therefore, with increasing cycles, an increase in W oxidation is observed along with a decrease in the O_2 reduction activity. After 10 cycles, however, both WC oxidation and O_2 reduction peaks stop shifting, and the system appears to reach a steady state.

Interestingly, when WC undergoes the same potential cycling, the extent of oxidation is almost equivalent to that of the ML Pt/WC, where the oxidation in the unmodified WC is 59%, comparing to a value of 66% for the ML Pt/WC after 15 CV cycles in O_2-saturated 0.5 M H_2SO_4. In previous studies for the methanol oxidation reaction, the Pt monolayer was found to protect the WC substrate from oxidation and increases its stability [9]. However, it seems that in the O_2-saturated electrolyte, this stability enhancement is not observed and ML Pt/WC exhibits a slightly higher extent of oxidation over uncovered WC. This might be because Pt can catalyze the oxidation of WC through relatively facile oxygen dissociation and subsequent spillover of the produced O from Pt onto WC.

Two reasons can account for the reduced activity of ML Pt/WC observed in Fig. 3. First, W-oxides can be a less active catalyst than WC. The effect of W-oxides on the ORR activity has not been explored previously in great detail, although there is evidence that Pt/WO_3 is less active than Pt/WC. Liu and Mustain have reported ORR polarization curves for Pt clusters on WC compared to Pt clusters on WO_3 and found that the Pt/WO_3 curve had both a more negative onset potential and a smaller limiting current [24] – both trends are observed in the current study. An

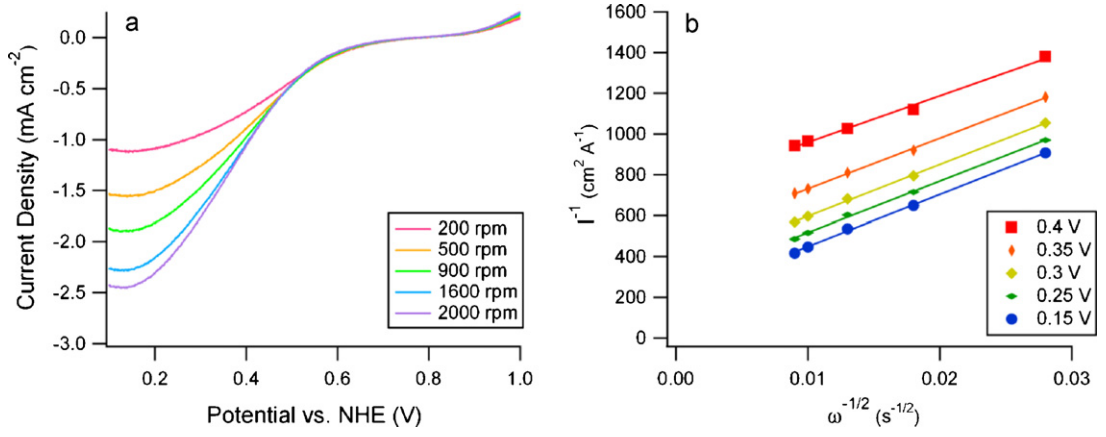

Fig. 7. (a) O_2 reduction polarization curves for Thick Pt/WC with varying rotation rate and (b) corresponding Koutecky–Levich plots.

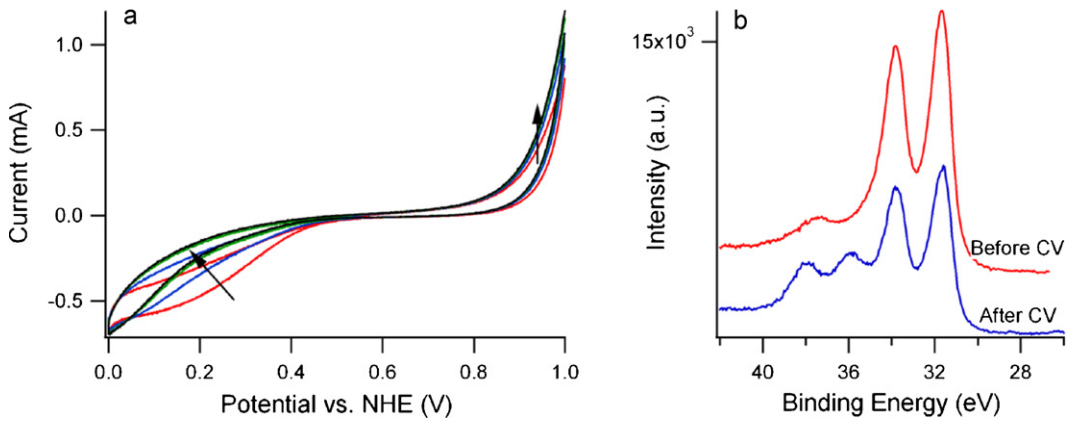

Fig. 8. (a) Cyclic voltammograms showing decreased activity for ML Pt/WC. Arrows indicate increasing cycles. (b) XPS spectra of W4f region before and after the CVs in part (a).

analogous example is Ru-based monolayer catalysts, which have been previously shown to be adversely affected by its susceptibility to irreversible oxidation [28]. When comparing ORR activities on Pt-modified Ru(0 0 0 1) and Pt-modified Ru(1 0 $\bar{1}$ 0), the Pt-modified Ru(0 0 0 1) was found to have more favorable results. The difference in activity was attributed to the fact that oxidation was more prevalent on Ru(1 0 $\bar{1}$ 0) than on Ru(0 0 0 1), with enhanced oxidation leading to the lower ORR activity [28].

The formation of W-oxides can also lead to the alteration of the Pt monolayer. Although the Pt overlayer is expected to protect the WC substrate from oxidation, as with methanol oxidation, the same effect does not appear to occur under ORR conditions. One possibility for the WC oxidation under the Pt monolayer is that oxygen diffuses through the Pt layer through its grain boundaries and then reacts with the WC substrate underneath at the higher oxidizing potentials. A similar phenomenon has been observed with thin Pt films evaporated on Si substrates. It has been found that oxygen can diffuse through Pt films up to 170 Å thick and react with the Si underlayer, forming a SiO_2 interfacial layer at elevated temperatures [29]. Increasing the Pt layer thickness also increases the O_2 diffusion barrier, which in turn reduces substrate oxidation [29]. Results from the current study suggest that the Pt monolayer becomes altered after the initial WC oxidation takes place, as indicated by the change in the Pt:W XPS ratio after the ORR measurements. If the monolayer was intact, then this ratio would remain constant. The Pt overlayer can either dissolve in solution or agglomerate to form larger particles. Both circumstances can cause a decline in activity such as that seen by the decreasing ORR peaks in Fig. 8a. The ORR activity has been found to be influenced both by particle size and by its crystalline structure in acid media [30]. Particle agglomeration can lead to decreased activity because of a loss of surface area, uncontrolled growth of the particle beyond the optimal size, or the growth of less efficient crystal planes. Furthermore, the increased oxidation of the WC after each cycle in Fig. 8a could result from the increased WC that is gradually exposed to the electrolyte as more Pt agglomerates or detaches from the surface.

4. Conclusions

In this work, the activity and stability of low-loading Pt on WC during the ORR have been elucidated. The use of well-defined WC disks ensures that the Pt monolayer makes intimate contact with the WC substrate, enabling the study of the Pt–WC interaction during the ORR. Other reports in the literature have used Pt–WC catalysts supported on carbon to study the effect of WC for the ORR, but the atomic arrangement of Pt and WC was unknown in these cases. The ML Pt/WC ORR polarization curve was found to have a more negative half-wave potential and smaller limiting current than that of a bulk Pt disk. The instability of the WC substrate under conditions of excess oxygen and high potentials prevents any activity enhancement from being observed on the ML Pt/WC system. It is believed that the oxidation of WC also affects the integrity of the Pt monolayer. When the WC surface is oxidized it can cause the Pt to either detach or agglomerate, both of which effectively ruin the effects of the monolayer Pt seen with other electrochemical reactions. Additionally, the reaction goes through the less efficient 2-electron process that produces the peroxide intermediate. Although it seems that one monolayer of Pt on WC does not aid in the ORR activity, it does not necessarily discount the positive results already witnessed in the previous literature under pH-potential regions where WC is electrochemically stable. The use of bulk Pt particles on tungsten carbides and tungsten oxides should continue to be studied, and the exact reasons for the observed ORR activity enhancement should be further explored.

Acknowledgements

We acknowledge financial support from the Department of Energy (DE-FG02-00ER15104). We also thank Mr. Daniel Esposito for discussion.

References

[1] J.K. Norskov, J. Rossmeisl, A. Logadottir, L. Lindqvist, J.R. Kitchin, T. Bligaard, H. Jonsson, J. Phys. Chem. B 108 (2004) 17886–17892.
[2] R.R. Adzic, J. Zhang, K. Sasaki, M.B. Vukmirovic, M. Shao, J.X. Wang, A.U. Nilekar, M. Mavrikakis, J.A. Valerio, F. Uribe, Top. Catal. 46 (2007) 249–262.
[3] M.B. Vukmirovic, J. Zhang, K. Sasaki, A.U. Nilekar, F. Uribe, M. Mavrikakis, R.R. Adzic, Electrochim. Acta 52 (2007) 2257–2263.
[4] J.L. Zhang, M.B. Vukmirovic, Y. Xu, M. Mavrikakis, R.R. Adzic, Angew. Chem. Int. Ed. 44 (2005) 2132–2135.
[5] D.V. Esposito, S.T. Hunt, A.L. Stottlemyer, K.D. Dobson, B.E. McCandless, R.W. Birkmire, J.G. Chen, Angew. Chem. Int. Ed. 49 (2010) 9859–9862.
[6] M.C. Weidman, D.V. Esposito, I.J. Hsu, J.G. Chen, J. Electrochem. Soc. 157 (2010) F179–F188.
[7] H.H. Hwu, J.G. Chen, Chem. Rev. 105 (2005) 185–212.
[8] Z.J. Mellinger, E.C. Weigert, A.L. Stottlemyer, J.G. Chen, Electrochem. Solid State Lett. 11 (2008) B63–B67.
[9] E.C. Weigert, A.L. Stottlemyer, M.B. Zellner, J.G. Chen, J. Phys. Chem. C 111 (2007) 14617–14620.
[10] I.J. Hsu, D.A. Hansgen, B.E. McCandless, B.G. Willis, J.G. Chen, J. Phys. Chem. C 115 (2011) 3709–3715.
[11] C. Liang, L. Ding, C. Li, M. Pang, D. Su, W. Li, Y. Wang, Energy Environ. Sci. 3 (2010) 1121–1127.
[12] Y. Liu, W.E. Mustain, ACS Catal. 1 (2010) 212–220.
[13] H. Meng, P.K. Shen, J. Phys. Chem. B 109 (2005) 22705–22709.
[14] H. Meng, P.K. Shen, Chem. Commun. (2005) 4408–4410.
[15] H. Meng, P.K. Shen, Z. Wei, S.P. Jiang, Electrochem. Solid State Lett. 9 (2006) A368–A372.
[16] M. Nie, P.K. Shen, M. Wu, Z.D. Wei, H. Meng, J. Power Sources 162 (2006) 173–176.

[17] L. Santos, K.S. Freitas, E.A. Ticianelli, J. Solid State Electrochem. 11 (2007) 1541–1548.
[18] M. Shao, B. Merzougui, K. Shoemaker, L. Stolar, L. Protsailo, Z.J. Mellinger, I.J. Hsu, J.G. Chen, J. Power Sources 196 (2011) 7426–7434.
[19] C. Song, J. Zhang, PEM Fuel Cell Electrocatalysts and Catalyst Layers: Fundamentals and Applications, Springer, London, 2008.
[20] Y. Wang, S.Q. Song, V. Maragou, P.K. Shen, P. Tsiakaras, Appl. Catal. B: Environ. 89 (2009) 223–228.
[21] X. Zhou, Y. Qiu, J. Yu, J. Yin, S. Gao, Int. J. Hydrogen Energy 36 (2011) 7398–7404.
[22] Q. Zhu, S.H. Zhou, X.Q. Wang, S. Dai, J. Power Sources 193 (2009) 495–500.
[23] H. Chhina, S. Campbell, O. Kesler, J. Power Sources 164 (2007) 431–440.
[24] H. Chhina, S. Campbell, O. Kesler, J. Power Sources 179 (2008) 50–59.
[25] W.E. Mustain, J. Prakash, J. Power Sources 170 (2007) 28–37.
[26] J. Lemaître, B. Vidick, B. Delmon, J. Catal. 99 (1986) 415–427.
[27] J.F. Moulder, W.F. Stickle, P.E. Sobol, K.D. Bomben, Handbook of X-ray Photoelectron Spectroscopy: A Reference Book of Standard Spectra for Identification and Interpretation of XPS Data, Physical Electronics, Inc., Eden Prairie, MN, 1995.
[28] H. Inoue, S.R. Brankovic, J.X. Wang, R.R. Adzic, Electrochim. Acta 47 (2002) 3777–3785.
[29] R. Schmiedl, V. Demuth, P. Lahnor, H. Godehardt, Y. Bodschwinna, C. Harder, L. Hammer, H.P. Strunk, M. Schulz, K. Heinz, Appl. Phys. A: Mater. 62 (1996) 223–230.
[30] N.M. Markovic, P.N. Ross, Surf. Sci. Rep. 45 (2002) 117–229.